1

Stretching & folding diagnostics in solutions of the three-dimensional Euler & Navier-Stokes equations

J. D. Gibbon and D. D. Holm
Department of Mathematics, Imperial College London, London, SW7 2AZ. UK.
j.d.gibbon@ic.ac.uk and d.holm@ic.ac.uk

Abstract

Two possible diagnostics of stretching and folding (S&F) in fluid flows are discussed, based on the dynamics of the gradient of potential vorticity ($q = \boldsymbol{\omega}\cdot\nabla\theta$) associated with solutions of the three-dimensional Euler and Navier-Stokes equations. The vector $\boldsymbol{\mathcal{B}} = \nabla q \times \nabla\theta$ satisfies the same type of stretching and folding equation as that for the vorticity field $\boldsymbol{\omega}$ in the incompressible Euler equations (Gibbon & Holm, 2010). The quantity θ may be chosen as the potential temperature for the stratified, rotating Euler/Navier-Stokes equations, or it may play the role of a seeded passive scalar for the Euler equations alone. The first discussion of these S&F-flow diagnostics concerns a numerical test for Euler codes and also includes a connection with the two-dimensional surface quasi-geostrophic equations. The second S&F-flow diagnostic concerns the evolution of the Lamb vector $\boldsymbol{D} = \boldsymbol{\omega}\times\boldsymbol{u}$, which is the nonlinearity for Euler's equations apart from the pressure. The curl of the Lamb vector ($\boldsymbol{\varpi} := \mathrm{curl}\,\boldsymbol{D}$) turns out to possess similar stretching and folding properties to that of the $\boldsymbol{\mathcal{B}}$-vector.

PACS numbers: 47.10.A-, 47.15.ki

1.1 Introduction

This paper considers two variants of the stretching and folding properties of gradients of solutions of the three-dimensional Euler and Navier-Stokes equations, following recent work of Gibbon & Holm (2010). Fine-scale structures, diagnosed in either inviscid or viscous turbulence and

MHD by the presence of large gradients, are created in the tortuous stretching and folding processes that arise from the vortex stretching term in the Euler and Navier-Stokes equations. These fine-scale structures are not wholly understood, as they lie at the heart of unsolved regularity issues that have challenged mathematicians for more than a generation.

In what follows the advected scalar field θ will comprise either : (i) the potential temperature for the stratified, rotating Euler/Navier-Stokes equations ; or (ii) a passive scalar for the Euler equations alone. The main theme revolves around the role of the vector $\boldsymbol{\mathcal{B}} = \nabla q \times \nabla\theta$ where the potential vorticity $q = \boldsymbol{\omega}\cdot\nabla\theta$ is conserved on fluid particle paths in either case. The basis of the result, already discussed by Kurgansky & Tatarskaya (1987) and Kurgansky & Pisnichenko (2000), is that in the incompressible Euler case the vector $\boldsymbol{\mathcal{B}}$ satisfies the same equation as that for the vorticity, thus suggesting intriguing stretching and folding properties for the gradient of the projection of $\boldsymbol{\omega}$ on the normal to level surfaces of θ. This result, summarized in §1.2, also has interesting consequences for the Navier-Stokes equations (Gibbon & Holm, 2010).

The first of the variants on this theme in §1.3.1 concerns a scheme for testing numerical Euler codes which have been designed to address the issue of whether the equations develop a finite time singularity. Thus it is apposite to devote the introduction to this section §1.3 to listing some of the Euler literature in this area. A closely associated problem forms the subject of §1.3.2 in which a connection is established with the two-dimensional surface quasi-geostrophic equations (2D-QG) studied by Constantin, Majda & Tabak (1994). In this $\nabla^{\perp}\theta$ in two-dimensions obeys the same vortex stretching equation as that of $\boldsymbol{\omega}$ for three-dimensional Euler. It is shown that the 2D-QG equations are embedded as a special case in the equation for $\boldsymbol{\mathcal{B}}$.

The second main variant revolves around the stretching and folding properties of the Lamb vector $\boldsymbol{D} = \boldsymbol{\omega}\times\boldsymbol{u}$ for the incompressible Euler equations. The Lamb vector comprises the nonlinearity of the Euler equations aside from the pressure, so its evolution is of importance. In §?? it is shown that its curl

$$\boldsymbol{\varpi} := \mathrm{curl}\,\boldsymbol{D} = \mathrm{curl}\,(\boldsymbol{\omega}\times\boldsymbol{u}) \tag{1.1}$$

also satisfies the same type of stretching equation as that for $\boldsymbol{\mathcal{B}}$, while its divergence ($\mathrm{div}\boldsymbol{D}$) obeys a continuity equation. In the compressible case this may have interesting consequences for the study of jet-noise although this is beyond the present scope of this paper. Section 1.4.2 deals with the evolution of the gradient of helicity density $\lambda = \boldsymbol{\omega}\cdot\boldsymbol{u}$ which also appears to possess similar stretching and folding properties.

Let us begin with the notation for the incompressible Euler equations, which are expressed as

$$\frac{D\boldsymbol{u}}{Dt} = -\nabla p\,, \quad \operatorname{div}\boldsymbol{u} = 0\,, \tag{1.2}$$

or as

$$\partial_t\boldsymbol{u} - \boldsymbol{u}\times\boldsymbol{\omega} = -\nabla\big(p + \tfrac{1}{2}u^2\big)\,. \tag{1.3}$$

The chosen domain is a three-dimensional periodic box $\mathcal{V} = [0, L]^3$. $\boldsymbol{u}$ is the velocity field of the fluid and the material derivative is defined by

$$\frac{D}{Dt} = \partial_t + \boldsymbol{u}\cdot\nabla\,. \tag{1.4}$$

The vorticity field $\boldsymbol{\omega} = \operatorname{curl}\boldsymbol{u}$ satisfies

$$\partial_t\boldsymbol{\omega} - \operatorname{curl}(\boldsymbol{u}\times\boldsymbol{\omega}) = 0\,. \tag{1.5}$$

This formula can also be written in the familiar vortex stretching format

$$\frac{D\boldsymbol{\omega}}{Dt} = \boldsymbol{\omega}\cdot\nabla\boldsymbol{u} \equiv \mathbf{S}\,\boldsymbol{\omega}\,, \tag{1.6}$$

where $\mathrm{S_{ij}} = \frac{1}{2}\left(\mathrm{u_{i,j}} + \mathrm{u_{j,i}}\right)$ is the rate of strain matrix. Equations (1.5) and (1.6) are equivalent evolution equations for $\boldsymbol{\omega}$. Euler data roughens very quickly, a fact which is mainly due to the **stretching and folding processes** caused by the rapid alignment or anti-alignment of $\boldsymbol{\omega}$ with positive and negative eigenvectors of $\mathbf{S}$.

The main aim of this paper is to show that these stretching and folding processes are shared by several other variables in the Euler and Navier-Stokes equations.

While the existence of some very weak solutions has been proved (Shnirelman, 1997; Brenier, 1999; Majda & Bertozzi, 2001; De Lellis & Székelyhidi, 2007, 2008; Brenier, De Lellis & Székelyhidi, 2009), nevertheless Leray-type weak solutions are unknown. However, if we are to progress in our understanding of the properties of solutions of the Euler equations, our lack of knowledge forces us to make some assumptions about the existence of solutions. The fundamental result on existence of solutions of the three-dimensional Euler equations is the theorem due to Beale, Kato & Majda (1984) which is assumed to hold :

Theorem 1.1.1 *(Beale, Kato & Majda, 1984) There exists a global solution* $\boldsymbol{u} \in C([0,\infty]; H^s) \cap C^1([0,\infty]; H^{s-1})$ *of the Euler equations for* $s \geq 3$ *if and only if, for every* $t > 0$,

$$\int_0^t \|\boldsymbol{\omega}(\cdot,\tau)\|_\infty \, d\tau < \infty\,. \tag{1.7}$$

Remarks. (i) The value of this result is that computationally only the quantity $\|\boldsymbol{\omega}\|_\infty$ needs to be monitored. If this is finite everywhere in the domain of flow at a time t then the solutions are regular at that time.

(ii) It does not predict a singularity in $\|\boldsymbol{\omega}\|_\infty$ but it restricts those that may potentially occur of the type $\|\boldsymbol{\omega}\|_\infty \sim (t_s - t)^{-p}$ to the range $p \geq 1$. When $p < 1$ the theorem is violated.

(iii) Kozono and Taniuchi (2000) have proved a version of this theorem in the BMO-norm (bounded mean oscillations) which is slightly weaker than the L^∞-norm.

(iv) Further analytical approaches have centred around conditional estimates on the magnitude and direction of vorticity that include the direction of vorticity. These are extensions of the Beale-Kato-Majda theorem ; the most significant papers are those by Constantin, Fefferman & Majda (1996), Deng, Hou & Yu (2005, 2006) and Chae (2003, 2004, 2005, 2007).

1.2 The $\mathcal{B}$ equation for the stratified Euler & Navier-Stokes equations

1.2.1 The stratified, rotating Euler equations

Let us consider the three-dimensional incompressible Euler equations for an incompressible, stratified, rotating flow ($\boldsymbol{\Omega} = \hat{\boldsymbol{k}}\,\Omega$) in terms of the velocity field $\boldsymbol{u}(\boldsymbol{x},t)$ and the potential temperature θ

$$\frac{D\boldsymbol{u}}{Dt} + 2\,(\boldsymbol{\Omega}\times\boldsymbol{u}) + a_0\hat{\boldsymbol{k}}\,\theta = -\nabla p\,, \tag{1.8}$$

where a_0 is a dimensionless constant and where $\theta(\boldsymbol{x},t)$ evolves passively according to

$$\frac{D\theta}{Dt} = 0\,. \tag{1.9}$$

How $\theta(\boldsymbol{x},t)$ and other variables might accumulate into large local concentrations is of interest[1]. To pursue this, consider the vorticity $\boldsymbol{\omega} =$

[1] The BKM theorem expressed in the last section is valid when θ is no more than a passive scalar driven by an Euler flow as in (1.5). For stratified Euler (1.8) together with (1.9), however, it is necessary to assume that $\int_0^t (\|\boldsymbol{\omega}\|_\infty + \|\nabla\theta\|_\infty)\, d\tau$ is finite.

curl $\boldsymbol{u}$ and define $\boldsymbol{\omega}_{rot} = \boldsymbol{\omega} + 2\boldsymbol{\Omega}$, which satisfies

$$\frac{D\,\boldsymbol{\omega}_{rot}}{Dt} = \boldsymbol{\omega}_{rot}\cdot\nabla\boldsymbol{u} - \nabla^{\perp}\theta \qquad\qquad \nabla^{\perp} = (\partial_y,\, -\partial_x,\, 0)\;. \tag{1.10}$$

The potential vorticity defined by (Hoskins, McIntyre & Robertson, 1985)

$$q = \boldsymbol{\omega}_{rot}\cdot\nabla\theta, \tag{1.11}$$

satisfies Ertel's theorem (Ertel, 1942; Truesdell & Toupin, 1960; Ohkitani, 1993; Kuznetsov & Zakharov, 1997) because

$$\begin{aligned}\frac{Dq}{Dt} &= \left(\frac{D\,\boldsymbol{\omega}_{rot}}{Dt} - \boldsymbol{\omega}_{rot}\cdot\nabla\boldsymbol{u}\right)\cdot\nabla\theta + \boldsymbol{\omega}_{rot}\cdot\nabla\left(\frac{D\theta}{Dt}\right)\\ &= -\nabla^{\perp}\theta\cdot\nabla\theta = 0\,.\end{aligned} \tag{1.12}$$

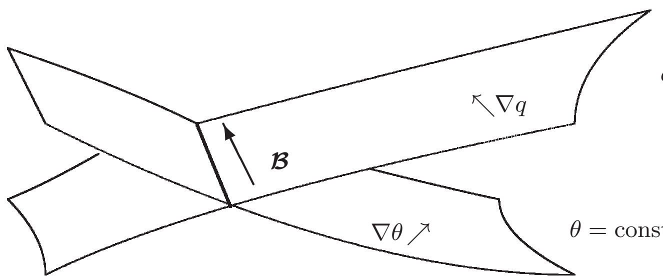

Fig. 1.1. The vector $\boldsymbol{\mathcal{B}}$ points along an intersection of level sets of the two Lagrangian flow constants $(q,\,\theta)$

.

This establishes two quantities q and θ that are each conserved along flow lines, and whose level sets intersect as in Figure 1.1. Then with $\boldsymbol{\mathcal{B}}$ defined as

$$\boldsymbol{\mathcal{B}} = \nabla q \times \nabla\theta \tag{1.13}$$

Kurgansky & Tartskaya (1987), Kurgansky & Pisnichenko (2000) have observed that $\boldsymbol{\mathcal{B}}$ satisfies[1]

$$\partial_t\boldsymbol{\mathcal{B}} = \mathrm{curl}\,(\boldsymbol{u}\times\boldsymbol{\mathcal{B}})\,. \tag{1.14}$$

[1]Note that this is a Clebsch representation of the divergence-free vector $\boldsymbol{\mathcal{B}}$, not a decomposition of the vorticity $\boldsymbol{\omega}$. See Ohkitani (2008) for a recent study of the latter and Holm & Kupershmidt (1983) for a review of the Clebsch approach. Moreover, the helicity of $\boldsymbol{\mathcal{B}}$ given by $\int_\Omega \boldsymbol{\mathcal{B}}\cdot \mathrm{curl}^{-1}\boldsymbol{\mathcal{B}}\,dV$ is necessarily zero for homogeneous or periodic boundary conditions.

Of course this may be written equivalently in the familiar vortex stretching format (1.6)

$$\frac{D\boldsymbol{\mathcal{B}}}{Dt} = \boldsymbol{\mathcal{B}} \cdot \nabla \boldsymbol{u} \tag{1.15}$$

thereby highlighting the fact that alignment of $\boldsymbol{\mathcal{B}}$ with eigenvectors of $\nabla \boldsymbol{u}$ is critical to the stretching process. In Figure 1.1 the vector $\boldsymbol{\mathcal{B}}$ is tangent to the curve defined by the intersection of q = const and θ = const. Thus, $\boldsymbol{\mathcal{B}}$ plays the same role as that for $\boldsymbol{\omega}$ and for the magnetic $\boldsymbol{B}$-field in MHD (Moffatt, 1978; Palmer, 1988). Hence, all the stretching and folding properties associated with vorticity or magnetic field-lines also apply to $\boldsymbol{\mathcal{B}}$ even though $\boldsymbol{\mathcal{B}}$ contains various projections of $\boldsymbol{\omega}$, $\nabla\boldsymbol{\omega}$, $\nabla\theta$ and $\nabla\nabla\theta$. Moreover, for any surface $S(\boldsymbol{u})$ moving with the flow $\boldsymbol{u}$, one finds

$$\frac{d}{dt}\int_{S(\boldsymbol{u})} \boldsymbol{\mathcal{B}} \cdot dS = 0\,. \tag{1.16}$$

1.2.2 The stratified Navier-Stokes equations

Now let us turn to the Navier-Stokes equations coupled to the θ-field. (In what follows the rotation will be ignored.) These equations are

$$\frac{D\boldsymbol{u}}{Dt} + a_0\theta\,\hat{\boldsymbol{k}} = Re^{-1}\Delta\boldsymbol{u} - \nabla p\,, \tag{1.17}$$

$$\frac{D\theta}{Dt} = \left(\sigma Re\right)^{-1}\Delta\theta\,. \tag{1.18}$$

Here, the potential vorticity $q = \boldsymbol{\omega}\cdot\nabla\theta$ is no longer a material constant but, instead, evolves according to

$$\begin{aligned}\frac{Dq}{Dt} &= \left(\frac{D\boldsymbol{\omega}}{Dt} - \boldsymbol{\omega}\cdot\nabla\boldsymbol{u}\right)\cdot\nabla\theta + \boldsymbol{\omega}\cdot\nabla\left(\frac{D\theta}{Dt}\right)\\ &= \left(Re^{-1}\Delta\boldsymbol{\omega} - \nabla^{\perp}\theta\right)\cdot\nabla\theta + \boldsymbol{\omega}\cdot\nabla\left[(\sigma Re)^{-1}\Delta\theta\right]\\ &= \mathsf{div}\left\{Re^{-1}\Delta\boldsymbol{u}\times\nabla\theta + (\sigma Re)^{-1}\boldsymbol{\omega}\Delta\theta\right\}.\end{aligned} \tag{1.19}$$

The material advection property is destroyed but the introduction of a *transport velocity field* $\boldsymbol{\mathcal{U}}_q$ transforms (1.19) into a continuity equation

$$\partial_t q + \operatorname{div}\left(q\boldsymbol{\mathcal{U}}_q\right) = 0\,, \tag{1.20}$$

thus making q a PV density, and where $\boldsymbol{\mathcal{U}}_q$ is defined through the relation

$$q\big(\boldsymbol{\mathcal{U}}_q - \boldsymbol{u}\big) = -Re^{-1}\big(\Delta\boldsymbol{u}\times\nabla\theta + \sigma^{-1}\boldsymbol{\omega}\Delta\theta\big)\,. \tag{1.21}$$

The introduction of the transport velocity field $\boldsymbol{\mathcal{U}}_q$ is originally due to Haynes & McIntyre (1987). Note that $\mathrm{div}\,\boldsymbol{\mathcal{U}}_q \neq 0$ although $\mathrm{div}\,\boldsymbol{\mathcal{U}}_q = O\,(Re)^{-1}$. Consistent with numerical studies on reconnection (Herring, Kerr & Rotunno 1994), this scaling with Reynolds number Re may suggest that in the early or intermediate stages of a flow this divergence may be small. What about the evolution of the variable θ? It is easily seen that

$$\begin{aligned}\partial_t\theta + \boldsymbol{\mathcal{U}}_q\cdot\nabla\theta &= \partial_t\theta + \boldsymbol{u}\cdot\nabla\theta - Re^{-1}q^{-1}\left\{\Delta\boldsymbol{u}\times\nabla\theta + \sigma^{-1}\boldsymbol{\omega}\Delta\theta\right\}\cdot\nabla\theta \\ &= \partial_t\theta + \boldsymbol{u}\cdot\nabla\theta - \left(\sigma Re\right)^{-1}\Delta\theta = \boldsymbol{0}\,. \end{aligned} \tag{1.22}$$

The formal result for the stratified Navier-Stokes equation is:

Theorem 1.2.1 *The scalar quantities q and θ satisfy*

$$\partial_t q + div\left(q\boldsymbol{\mathcal{U}}_q\right) = 0\,, \qquad \partial_t\theta + \boldsymbol{\mathcal{U}}_q\cdot\nabla\theta = 0\,, \tag{1.23}$$

and $\boldsymbol{\mathcal{B}} = \nabla q\times\nabla\theta$ satisfies the stretching and folding relation

$$\partial_t\boldsymbol{\mathcal{B}} - curl(\boldsymbol{\mathcal{U}}_q\times\boldsymbol{\mathcal{B}}) = \boldsymbol{\mathcal{D}}_q\,, \tag{1.24}$$

where the divergence-less vector $\boldsymbol{\mathcal{D}}_q$ is given by

$$\boldsymbol{\mathcal{D}}_q = -\nabla(q\,div\boldsymbol{\mathcal{U}}_q)\times\nabla\theta\,, \tag{1.25}$$

and the transport velocity $\boldsymbol{\mathcal{U}}_q$ is defined as in (1.21). Moreover, for any surface $\boldsymbol{S}(\boldsymbol{\mathcal{U}}_q)$ moving with the flow $\boldsymbol{\mathcal{U}}_q$

$$\frac{d}{dt}\int_{\boldsymbol{S}(\boldsymbol{\mathcal{U}}_q)}\boldsymbol{\mathcal{B}}\cdot d\boldsymbol{S} = \int_{\boldsymbol{S}(\boldsymbol{\mathcal{U}}_q)}\boldsymbol{\mathcal{D}}_q\cdot d\boldsymbol{S}\,. \tag{1.26}$$

This is the natural way of expressing problems in the vortex stretching format using the transport velocity $\boldsymbol{\mathcal{U}}_q$.

1.3 The Euler singularity problem

Out of large-scale computations of solutions of the three dimensional Euler equations has emerged the natural question of whether a singularity develops in a finite time (Majda & Bertozzi, 2001; Bardos & Titi, 2007; Constantin, 2008; Gibbon, 2008). An extensive literature has arisen on this question but no conclusion has yet been agreed: see Bardos & Benachour (1977); Morf, Orszag & Frisch (1980); Chorin (1982), Brachet, Meiron, Orszag, Nickel, Morf & Frisch (1983); Siggia (1984); Kida (1985); Ashurst & Meiron (1987); Pumir & Kerr, (1987); Pumir & Siggia (1990); Grauer & Sideris (1991); Bell & Marcus (1992); Brachet, Meneguzzi, Vincent, Politano & Sulem (1992); Kerr (1993, 2005a, 2005b); Boratav & Pelz (1994, 1995); Pelz (1997, 2001); Pelz & Gulak (1997); Grauer, Marliani & Germaschewski (1998); Cichowlas & Brachet (2005); Gulak & Pelz (2005); Pelz & Ohkitani (2005); Pauls, Matsumoto, Frisch & Bec (2006). Regarding more recent work, the fine-scale computations by Hou and Li (2006, 2007) that see only super-exponential growth in $\boldsymbol{\omega}$ contradict both the older computations of Kerr (1993, 2005a) together with newer results by Bustamante and Kerr (2007), in which a finite time singularity has been observed. Similar but not identical anti-parallel vortex tube initial conditions have been used in the two bodies of results which largely coincide until a late stage. Two further recent contributions are those of Orlandi and Carnevale (2007) who used initial conditions in the form of Lamb dipoles to observe singular behaviour, as did Grafke, Homann, Dreher & Grauer (2007).

1.3.1 A numerical test for Euler computations

Let us take the Euler equations for the velocity field $\boldsymbol{u}$ in their standard form as in (1.2) without the rotation or buoyancy used in §1.2. The new feature of the proposed test is to introduce a passive tracer concentration $\theta(\boldsymbol{x},\,t)$ satisfying

$$\frac{D\theta}{Dt} = 0\,, \tag{1.27}$$

and whose initial data are under the investigator's control. Introducing θ allows us, as before, to use $q = \boldsymbol{\omega}\cdot\nabla\theta$ which still obeys

$$\frac{Dq}{Dt} = 0\,, \tag{1.28}$$

and which therefore allows the use of the same definition $\boldsymbol{\mathcal{B}} = \nabla q \times \nabla\theta$. This is endowed with initial conditions inherited from those for $\boldsymbol{u}$ and θ. $\boldsymbol{\mathcal{B}}$ must satisfy

$$\partial_t \boldsymbol{\mathcal{B}} = \mathrm{curl}\,(\boldsymbol{u}\times\boldsymbol{\mathcal{B}}) \qquad \text{or} \qquad \frac{D\boldsymbol{\mathcal{B}}}{Dt} = \boldsymbol{\mathcal{B}}\cdot\nabla\boldsymbol{u}\,, \tag{1.29}$$

which mimics the vorticity stretching equation (1.5). The critical point about the use of the vector field $\boldsymbol{\mathcal{B}}$ is that it has embedded information on $\boldsymbol{\omega}$, $\nabla\boldsymbol{\omega}$, $\nabla\theta$ and $\nabla\nabla\theta$. It evolves in the same way as $\boldsymbol{\omega}$ and so is subjected to similar stretching and folding processes. It can, however, be evaluated at any particular time t in several distinct ways: it can be evaluated from the result of the evolution in (1.29) at time t, or it can be computed from its definition using $\boldsymbol{u}$ and θ evolved up to and evaluated at time t. The degree to which these distinct evaluations agree or disagree provides a quantitative gauge of the accuracy of the numerical computation. It is not clear that there is a natural scale for the inevitable discrepancies produced in any particular computation. However, this procedure produces a precise diagnostic quantity that, given identical initial data, can be directly compared side-by-side for different numerical computations to evaluate their *relative* accuracy. The suggested test is:

(i) Choose initial data for $\boldsymbol{u}$ and θ, thereby fixing initial data for q and $\boldsymbol{\mathcal{B}}$.

(ii) Evolve $\boldsymbol{u}$ and simultaneously solve $D\theta/Dt = 0$, $Dq/Dt = 0$ and $D\boldsymbol{\mathcal{B}}/Dt = \boldsymbol{\mathcal{B}} \cdot \nabla\boldsymbol{u}$.

(iii) Test the resolution at any time $t > 0$ by constructing $q_1(\cdot\,,\,t) = \boldsymbol{\omega}(\cdot\,,\,t) \cdot \nabla\theta(\cdot\,,\,t)$ and then:

(a) compare the solution for $\boldsymbol{\mathcal{B}}(\cdot, t)$ obtained from solving the stretching equation $D\boldsymbol{\mathcal{B}}/Dt = \boldsymbol{\mathcal{B}} \cdot \nabla\boldsymbol{u}$ with

$$\boldsymbol{\mathcal{B}}_1(\cdot\,,\,t) = \nabla q_1(\cdot\,,\,t) \times \nabla\theta(\cdot\,,\,t) \tag{1.30}$$

(b) Furthermore, compare this with

$$\boldsymbol{\mathcal{B}}_2(\cdot\,,\,t) = \nabla q\,(\cdot\,,\,t) \times \nabla\theta(\cdot\,,\,t) \tag{1.31}$$

where $q\,(\cdot\,,\,t)$ is the evolved solution of $Dq/Dt = 0$.

(iv) For fixed initial data for $\boldsymbol{u}$ this procedure may be implemented for a variety of "markers" $\theta_n(\cdot\,,\,t)$ evolving from distinct initial data $\theta_n(\cdot\,,\,0)$ to diagnose the numerical accuracy in different regions of the flow.

Because $\boldsymbol{\mathcal{B}}$ contains $\nabla\boldsymbol{\omega}$, comparing the different computations of $\boldsymbol{\mathcal{B}}$, $\boldsymbol{\mathcal{B}}_1$ and $\boldsymbol{\mathcal{B}}_2$ tests the accuracy of the computation of some of the small scale structures in the flow. Given the generally acknowledged difficulties in accurately computing the evolution of passive scalars such as in (1.27) or (1.28), how initial data are chosen may be critical to the calculation. In particular, the appearance of null points in the vorticity field may create significant obstacles – see Ohkitani (2008).

1.3.2 Connection with the two-dimensional quasi-geostrophic equations

The open nature of whether the three dimensional Euler equations develops a singularity naturally leads to the idea of studying other simpler problems that mimic this behaviour. The foremost example is the case of the two dimensional surface quasi-geostrophic (2D-QG) equations. The strong fronts observed in numerical computations though the existence of a vortex stretching term have led Constantin, Majda & Tabak (1994) to suggest that these might model singularity development in the three dimensional Euler equations. It turns out that the 2D-QG equations are embedded in the equation for $\boldsymbol{\mathcal{B}}$ in the following way.

Let $q = z =$ const and $\theta =$ const be material surfaces. Then $\boldsymbol{\mathcal{B}}$ becomes

$$\boldsymbol{\mathcal{B}} = \nabla z \times \nabla\theta = \hat{\boldsymbol{k}} \times \nabla\theta = -\nabla^{\perp}\theta\,. \tag{1.32}$$

So far the velocity field has been left $\boldsymbol{u}$ free but if this is then chosen such that in $\mathbb{R}^2$

$$\boldsymbol{u} = -\nabla^{\perp}\psi \qquad \text{with} \qquad \theta = -(-\Delta)^{1/2}\psi \tag{1.33}$$

then the equations for $\boldsymbol{\mathcal{B}}$ with this $\boldsymbol{u}$ satisfies

$$\frac{D\boldsymbol{\mathcal{B}}}{Dt} = \boldsymbol{\mathcal{B}}\cdot\nabla\boldsymbol{u}\,. \tag{1.34}$$

These are the 2D-QG equations discussed by Constantin, Majda & Tabak (1994) who linked the formation of a singularity to the a presence of hyperbolic saddle (for the level sets). Córdoba (1998) then showed the absence of a singularity in the case of a *simple* hyperbolic saddle. We refer the reader to for related work connected to the formation of sharp fronts and their evolution: Ohkitani & Yamada (1997) Constantin, Nie & Schorghofer (1998), Córdoba (1998), Córdoba, Fefferman & Rodrigo (2004) & Rodrigo (2004).

1.4 Transport equations for the curl and divergence of the Lamb vector

For both the incompressible and compressible Euler equations, apart from the non-local effects of the pressure, the nonlinearity is the *Lamb vector*

$$\boldsymbol{D} = \boldsymbol{\omega} \times \boldsymbol{u}\,. \tag{1.35}$$

This is the cross product of vorticity and velocity and is therefore an indicator of regions of a flow field where vorticity is nonzero. It shares its critical points with velocity and vorticity, but possesses additional critical points where the flow is locally Beltrami, as in the helical motion of a swirling jet. The evolution of $\boldsymbol{D}$ is of interest: its divergence, for example, plays a role in the production of jet-noise in compressible flows, wherever the mean of $\operatorname{div}\boldsymbol{D} \neq 0$. For recent discussions of the utility of the this vector as a diagnostic in fluid dynamics or as an important source of jet noise, see Rousseaux, Seifer, Steinberg & Wiebel (2007), Hamman, Klewick & Kirby (2008) and Cabana, Fortuné & Jordan (2008), respectively. In the incompressible case, existence of solutions is assured provided the Beale, Kato, Majda (1984) condition is fulfilled.

1.4.1 The evolution of D for the incompressible Euler equations

In the case of the incompressible Euler equations, we distinguish the Lamb vector $\boldsymbol{D} = \boldsymbol{\omega} \times \boldsymbol{u}$ from the ***Bernoulli vector***

$$\boldsymbol{E} = \boldsymbol{D} + \nabla(p + \tfrac{1}{2}u^2)\,. \tag{1.36}$$

The incompressible Euler fluid equations (1.3) are connected to $\boldsymbol{D}$ and $\boldsymbol{E}$ by

$$\partial_t \boldsymbol{u} = -\,\boldsymbol{D} - \nabla(p + \tfrac{1}{2}u^2) = -\,\boldsymbol{E}\,, \tag{1.37}$$

which vanishes for steady flows to create Lamb surfaces, reviewed, e.g., in Sposito (1997). The Bernoulli vector $\boldsymbol{E}$ is distinguished from the Lamb vector $\boldsymbol{D}$ by its divergence, in that

$$\operatorname{div}\boldsymbol{E} = 0\,, \quad \text{while in general} \quad \operatorname{div}\boldsymbol{D} \neq 0\,, \tag{1.38}$$

although they both share the same curl, i.e., $\operatorname{curl}\boldsymbol{E} = \operatorname{curl}\boldsymbol{D} = \boldsymbol{\varpi}$. We now choose to rewrite the vorticity equation (1.5) as

$$\partial_t \boldsymbol{\omega} + \operatorname{curl}\boldsymbol{E} = 0\,, \tag{1.39}$$

and thereby remove any gauge freedom in the curl^{-1} operation. That is, we choose the *Bernoulli gauge*, in which $\operatorname{curl}^{-1}\boldsymbol{\varpi} = \boldsymbol{E}$.

The aim of this section is to show that the curl of the Lamb vector $\boldsymbol{\varpi} = \operatorname{curl}\boldsymbol{E}$ plays a role similar to that of $\boldsymbol{\mathcal{B}}$ in Theorem 1.2.1 and its divergence $\operatorname{div}\boldsymbol{D}$ obeys a conservation equation that introduces an augmented transport velocity field, in the same spirit as in Haynes & McIntyre (1987).

The Euler fluid equations imply the following equation for the evolution of the Lamb vector,

$$\partial_t \boldsymbol{D} - \boldsymbol{u} \times \boldsymbol{\varpi} \;=\; \boldsymbol{E} \times \boldsymbol{\omega}\,, \tag{1.40}$$

and so

Theorem 1.4.1 $\boldsymbol{\varpi} = \operatorname{curl} \boldsymbol{E}$ *satisfies the stretching equation*

$$\partial_t \boldsymbol{\varpi} - \operatorname{curl}(\boldsymbol{u} \times \boldsymbol{\varpi}) \quad = \quad \boldsymbol{\mathcal{D}}_{lam} \,, \tag{1.41}$$

where $\boldsymbol{\mathcal{D}}_{lam}$ *is defined by*

$$\boldsymbol{\mathcal{D}}_{lam} = \operatorname{curl}(\boldsymbol{E} \times \boldsymbol{\omega}),$$

and $\operatorname{div} \boldsymbol{D}$ *satisfies the conservation equation*

$$\partial_t (\operatorname{div} \boldsymbol{D}) + \operatorname{div}\big[\boldsymbol{\mathcal{U}}(\operatorname{div}\boldsymbol{D})\big] = 0 \,, \tag{1.42}$$

where the transport velocity $\boldsymbol{\mathcal{U}}$ *is defined by*

$$(\boldsymbol{\mathcal{U}} - \boldsymbol{u}) \operatorname{div} \boldsymbol{D} = \boldsymbol{u} \times (2\boldsymbol{S} \cdot \boldsymbol{\omega}) + \boldsymbol{\omega} \times \nabla(p + \tfrac{1}{2}u^2) \,, \tag{1.43}$$

and $\boldsymbol{S}$ *is the strain-rate tensor.*

Remarks: This theorem is similar in spirit to Theorem 1.2.1 for the evolution of $\boldsymbol{\mathcal{B}}$ and the continuity equation for q, with $\boldsymbol{\varpi}$ and $\operatorname{div} \boldsymbol{D}$ playing these roles respectively. Four further observations about these equations follow that all hinge of the property that $\operatorname{div} \boldsymbol{E} = 0$.

(1) Another expression for the divergence of the Lamb vector is

$$\operatorname{div}\boldsymbol{D} = -\,\Delta(p + \tfrac{1}{2}u^2) \,. \tag{1.44}$$

Therefore, equation (1.42) is conceivably interesting as an evolution equation for the Bernoulli function $\big(p + \frac{1}{2}u^2\big)$. In compressible turbulence, such as in the exhaust of a jet airplane, the jet noise is largely due to correlations that produce a mean $\operatorname{div}\boldsymbol{D} \neq 0$, as discussed in Cabana, Fortuné & Jordan (2008). That is, the divergence of the Lamb vector is the leading source of turbulent jet noise, so the conservation equation (1.42) for its evolution in the incompressible case may be of interest. The quantity in square brackets in (1.42) is the *current density* for the transport of the *hydrodynamic charge density*, $\operatorname{div}\boldsymbol{D} = -\,\Delta\big(p + \frac{1}{2}u^2\big)$.

(2) Because $\operatorname{div} \boldsymbol{E} = 0$, the Helmholtz equation (1.39) and the curl of (1.41), rewritten as

$$\boldsymbol{\varpi}_t - \operatorname{curl}(\boldsymbol{u} \times \boldsymbol{\varpi}) \quad = \quad \operatorname{curl}(\boldsymbol{E} \times \boldsymbol{\omega}) \,, \tag{1.45}$$

imply the following two-component system of commutator equations

$$\boldsymbol{\varpi}_t + [\boldsymbol{u}, \boldsymbol{\varpi}] \quad = \quad [\boldsymbol{\omega}, \operatorname{curl}^{-1}\boldsymbol{\varpi}], \tag{1.46}$$

$$\partial_t \boldsymbol{\omega} + [\boldsymbol{u}, \boldsymbol{\omega}] \quad = \quad 0 \,, \quad \text{where} \quad \boldsymbol{u} = \operatorname{curl}^{-1}\boldsymbol{\omega} \tag{1.47}$$

and we have $\boldsymbol{E} = \mathrm{curl}^{-1}\boldsymbol{\varpi}$ in the Bernoulli gauge. The bracket $[\,\cdot\,,\,\cdot\,]$ in these equations denotes commutator of divergence-free vector fields. For example,

$$[\boldsymbol{\omega},\,\boldsymbol{E}] := \boldsymbol{\omega}\cdot\nabla\boldsymbol{E} - \boldsymbol{E}\cdot\nabla\boldsymbol{\omega}. \tag{1.48}$$

(3) Given that $\mathrm{div}\,\boldsymbol{E} = 0$, one may compute the evolution of $\boldsymbol{E}$-*helicity*, defined as

$$\Lambda_E := \int \boldsymbol{E}\cdot d\mathbf{x}\wedge d(\boldsymbol{E}\cdot d\mathbf{x}) = \int \boldsymbol{E}\cdot\,\mathrm{curl}\,\boldsymbol{E}\,dV\,. \tag{1.49}$$

Equations (1.41) and (1.40) imply that the helicity of $\boldsymbol{E}$ is not constant. Instead, Λ_E evolves as

$$\frac{d}{dt}\int \boldsymbol{E}\cdot\,\mathrm{curl}\,\boldsymbol{E}\,dV = -\,2\int \boldsymbol{\omega}\cdot\left(\boldsymbol{E}\times\mathrm{curl}\,\boldsymbol{E}\right)\,dV\,, \tag{1.50}$$

after integrating by parts to remove gradient terms and applying homogeneous boundary conditions.

(4) Finally, we remark that the steps taken to distinguish between the fields $\boldsymbol{D}$ and $\boldsymbol{E}$ in selecting the Bernoulli gauge etc. are all reminiscent of a formal Eulerian analogy with Maxwell's equations for electromagnetism. All that remains in completing that well-known formal analogy is to identify $\boldsymbol{\omega}$ with the magnetic field $\boldsymbol{B}$ and require the curl of the magnetic induction $\boldsymbol{H}$ to vanish, i.e., $\mathrm{curl}\,\boldsymbol{H} = 0$. Then one may interpret $\partial_t\boldsymbol{D}$ in equation (1.40) as the displacement current, the right hand side as the current density, etc. . This is slightly different from the variant of that formal analogy discussed previously in Marmanis (1998) and pursued in fluid experiments by Rousseaux, Seifer, Steinberg & Wiebel (2007). For completeness, we list the comparison in Table 1.2.

Maxwell's equations	Marmanis (1998)	Present paper
Magnetic Field, $\boldsymbol{B}$	$\boldsymbol{\omega} = \mathrm{curl}\,\boldsymbol{u}$	$\boldsymbol{\omega} = \mathrm{curl}\,\boldsymbol{u}$
Magnetic Induction, $\boldsymbol{H}$	Absent	$\nabla\chi$
Electric Field, $\boldsymbol{E}$	$\boldsymbol{\omega}\times\mathbf{u}$	$\boldsymbol{\omega}\times\boldsymbol{u} + \nabla(p + \frac{1}{2}u^2)$
Displacement vector, $\boldsymbol{D}$	Absent	$\boldsymbol{\omega}\times\boldsymbol{u}$
Charge density, q_E	$\mathrm{div}\,(\boldsymbol{\omega}\times\boldsymbol{u})$	$\mathrm{div}\,(\boldsymbol{\omega}\times\boldsymbol{u})$

Fig. 1.2. Compared with Marmanis (1998), the current Maxwell-hydrodynamics analogy distinguishes between $(\boldsymbol{E},\boldsymbol{B})$ and $(\boldsymbol{D},\boldsymbol{H})$.

We shall refrain, however, from following the formal analogy between hydrodynamics and Maxwell equations here, and finish by interpreting the transport theorems for the Lamb vector's divergence (1.42) and its curl (1.45) in the standard fluid context.

In the fluid context, we interpret the commutator equations (1.46) and (1.47) as evolution equations for the Lagrangian fluxes $\boldsymbol{\varpi} \cdot d\boldsymbol{S}$ and $\boldsymbol{\omega} \cdot d\boldsymbol{S}$ as they are swept along by the fluid velocity $\boldsymbol{u}$. Namely,

$$\frac{d}{dt}(\boldsymbol{\varpi} \cdot d\boldsymbol{S}) \quad = \quad \text{curl}\big(\boldsymbol{E} \times \boldsymbol{\omega}\big) \cdot d\boldsymbol{S} \tag{1.51}$$

$$\frac{d}{dt}(\boldsymbol{\omega} \cdot d\boldsymbol{S}) \quad = \quad 0\,, \tag{1.52}$$

both along $d\boldsymbol{x}(t)/t = \boldsymbol{u}(\boldsymbol{x}(t), t)$. As always, the Helmholtz equation (1.52) states that the flux of vorticity is frozen into the flow. However, the flux of the cross product of vorticity and the Bernoulli vector drives the flux of the the Lamb vector's curl, which in turn drives the evolution of the vorticity. In a nonlinear feedback response, the Lamb vector's curl is driven itself in equation (1.51) by the flux of the vector product of the vorticity with the Bernoulli vector, which contains *both* the nonlinearity and the pressure gradient. This process is akin to a magnetic dynamo, with the vorticity playing the role of the magnetic field.

One may also express this process as a pair of linked circulation theorems, namely,

$$\frac{d}{dt}\oint_{c(\boldsymbol{u})} \boldsymbol{E} \cdot d\boldsymbol{x} \quad = \quad \oint_{c(\boldsymbol{u})} \big(\boldsymbol{E} \times \boldsymbol{\omega}\big) \cdot d\boldsymbol{x} \tag{1.53}$$

$$\frac{d}{dt}\oint_{c(\boldsymbol{u})} \boldsymbol{u} \cdot d\boldsymbol{x} \quad = \quad 0\,, \tag{1.54}$$

where $c(\boldsymbol{u})$ is a closed material loop moving with the fluid velocity $\boldsymbol{u}$. Thus, the circulation of the Lamb vector (or the Bernoulli vector) is driven by the circulation of the cross product of the Bernoulli vector with the vorticity.

In addition, the Lamb vector's divergence ($\text{div}\,\boldsymbol{D}$) satisfies the continuity equation (1.43) with its augmented transport velocity that depends on the vorticity, the strain-rate tensor and the pressure gradient.

1.4.2 Helicity density

Having looked at the dynamics of the Lamb vector $\boldsymbol{D} = \boldsymbol{\omega} \times \boldsymbol{u}$ let us consider the helicity density of the Euler equations which is the scalar product

$$\lambda = \boldsymbol{\omega} \cdot \boldsymbol{u} \,. \tag{1.55}$$

Straightforward differentiation gives its dynamical equation,

$$\frac{D\lambda}{Dt} = -\boldsymbol{\omega} \cdot \nabla \left(p - \tfrac{1}{2} u^2 \right) \tag{1.56}$$

which may be rewritten equivalently as

$$\partial_t \lambda + \operatorname{div} \left\{ \lambda \boldsymbol{u} + \boldsymbol{\omega} \left(p - \tfrac{1}{2} u^2 \right) \right\} = 0 \,. \tag{1.57}$$

As in §1.2, this leads to the definition of a transport velocity field $\boldsymbol{\mathcal{U}}_\lambda$

$$\lambda (\boldsymbol{\mathcal{U}}_\lambda - \boldsymbol{u}) = \boldsymbol{\omega} \left(p - \tfrac{1}{2} u^2 \right) \tag{1.58}$$

and the continuity equation

$$\partial_t \lambda + \operatorname{div}(\lambda \boldsymbol{\mathcal{U}}_\lambda) = 0 \,. \tag{1.59}$$

Thus, the vector quantity

$$\boldsymbol{\mathcal{B}}_\lambda = \nabla \lambda \times \nabla \theta \tag{1.60}$$

satisfies the stretching and folding result of Theorem 1.2.1 of §1.2

$$\partial_t \boldsymbol{\mathcal{B}}_\lambda - \operatorname{curl} (\boldsymbol{u} \times \boldsymbol{\mathcal{B}}_\lambda) = \boldsymbol{\mathcal{D}}_\lambda \,, \tag{1.61}$$

with vector $\boldsymbol{\mathcal{D}}_\lambda$ defined as

$$\boldsymbol{\mathcal{D}}_\lambda = -\nabla \left(\lambda \operatorname{div} \boldsymbol{\mathcal{U}}_\lambda \right) \times \nabla \theta \,. \tag{1.62}$$

The vector $\boldsymbol{\mathcal{D}}_\lambda$ measures the "permeability" or rate of slippage of level sets of helicity density through level sets of the passive scalar field, θ.

1.5 Conclusion

The stretching and folding processes that produce small-scale structures in either fluid turbulence or MHD have generally been associated with the alignment or anti-alignment of either the vorticity $\boldsymbol{\omega}$ or the magnetic field $\boldsymbol{B}$ with eigenvectors of the velocity gradient matrix $\nabla \boldsymbol{u}$. The observations and calculations in this paper have shown that these stretching and folding processes occur quite widely : on the one hand they have been shown to apply to any system that involves two passive scalars riding on a flow $\boldsymbol{u}$, such as (q, θ) for the stratified, rotating Euler and Navier-Stokes equations, while on the other hand both the curl of the Lamb vector and the helicity density $\lambda = \boldsymbol{\omega} \cdot \boldsymbol{u}$ for incompressible flow also possess this behaviour. The significant feature is that we are one gradient higher on $\boldsymbol{\omega}$ itself. The embedded gradient of $\boldsymbol{\omega}$ within $\boldsymbol{\mathcal{B}}$ has been identified as the basis of a test for Euler codes, as explained in §1.3.1.

That the Lamb vector fits into this stretching and folding picture is a surprise. It is generally associated with studies in jet-noise in aero-acoustics and its natural context is compressible flows in which wave motion is observed, However, because it is the kinematic nonlinearity of fluid flow its evolution is important in also characterizing incompressible fluid motion. The stretching and folding process turns out to fit into an electro-magnetic analogy. We hope this analogy may become useful in transferring methods of mimetic difference schemes that are highly developed for electro-magnetic applications into the arena of Eulerian fluid dynamics. Mimetic methods are reviewed, for example, in Lipnikov, Shashkov & Yotov (2009).

Acknowledgements: The authors thank Colin Cotter, Charles Doering, Edriss Titi and Claude Bardos for helpful discussions.

References

Ashurst, W. & Meiron, D. (1987) Numerical study of vortex reconnection. *Phys. Rev. Lett.* **58**, 1632-1635.

Bardos, C. (1972) Existence et unicité de la solution de l'équation d'Euler en dimension deux. *J. Math. Anal. Appl.* **40**, 769-790.

Bardos, C., Benachour, S. & Zerner, M. (1976) Analyticité des solutions périodiques de l'équation d'Euler en deux dimensions. *C. R. Acad. Sc. Paris* **282A** 995-998.

Bardos, C. & Benachour, S. (1977) Domaine d'analyticité des solutions de l'équation d'Euler dans un ouvert de $\mathbb{R}^n$. *Ann. Sc. Norm. Super. Pisa, Cl. Sci.* IV Ser., **4** 647–687.

Bardos, C. & Titi, E. S. (2007) Euler equations of incompressible ideal fluids. *Russ. Math. Surv.* **62:3**, 409–451.

Beale, J. T., Kato, T. & Majda, A. J. (1984) Remarks on the breakdown of smooth solutions for the 3D Euler equations. *Commun. Math. Phys.* **94**, 61-66.

Bell, J. B. & Marcus, D. L. (1992) Vorticity intensification and transition to turbulence in the three-dimensional Euler equations. *Comm. Math. Phys.* **147**, 371–394.

Boratav, O. N. & Pelz, R. B. (1994) Direct numerical simulation of transition to turbulence from a high-symmetry initial condition. *Phys. Fluids* **6**, 2757–2784.

Boratav, O. N. & Pelz, R. B. (1995) On the local topology evolution of a high-symmetry flow. *Phys. Fluids* **7**, 1712–1731.

Brachet, M. E., Meiron, D. I., Orszag, S. A., Nickel, B. G., Morf, R. H & Frisch, U. (1983) Small-scale structure of the Taylor–Green vortex. *J. Fluid Mech.* **130**, 411-452.

Brachet, M. E., Meneguzzi, V., Vincent, A., Politano, H. & Sulem, P.-L. (1992) Numerical evidence of smooth self-similar dynamics and the possibility of subsequent collapse for ideal flows. *Phys. Fluids* **4A**, 2845-2854.

Brenier, Y. (1999) Minimal geodesics on groups of volume-preserving maps and generalized solutions of the Euler equations. *Comm. Pure Appl. Math.* **52**, 411-452.

Brenier, Y., De Lellis, C. & Székelyhidi, L. (2009) Weak-strong uniqueness for measure-valued solutions. arXiv:0912.1028v1

Bustamante, M. D. & Kerr, R. M. (2008) *3D Euler about a 2D Symmetry Plane*, Proc. of "Euler Equations 250 years on" Aussois June 2007, *Physica D* **237,** 1912–1920.

Cabana, M., Fortuné, V. & Jordan, P. (2008) Identifying the radiating core of Lighthill's source term. *Theor. Comput. Fluid Dyn.* **22** 87-106.

Chae, D. (2003) Remarks on the blow-up of the Euler equations and the related equations, *Comm. Math. Phys.* **245**, 539-550.

Chae, D. (2004) Local Existence and Blow-up Criterion for the Euler Equations in the Besov Spaces. *Asymptotic Analysis* **38**, 339-358.

Chae, D. (2005) Remarks on the blow-up criterion of the 3D Euler equations *Nonlinearity* **18**, 1021-1029.

Chae, D. (2007) On the finite time singularities of the 3D incompressible Euler equations. Comm. Pure App. Math. **60**, 597-617.

Chorin, A. J. (1982) The evolution of a turbulent vortex. *Commun. Math. Phys.* **83**, 517–535.

Cichowlas, C. & Brachet, M.-E. (2005) Evolution of complex singularities in Kida-Pelz and Taylor-Green inviscid flows. *Fluid Dyn. Res.* **36**, 239-248.

Constantin, P. & Foias, C. (1988) *Navier-Stokes Equations*, The University of Chicago Press, Chicago.

Constantin, P. (1994) Geometric statistics in turbulence. *SIAM Rev.* **36** 73-98

Constantin, P. (1992) Regularity results for incompressible fluids. *Proceedings to the Workshop on the Earth Climate as a Dynamical System, Argonne National Laboratory*, (ANL/MCSTM-170) 25–26, (September 1992).

Constantin, P., Fefferman, Ch. & Majda A. J. (1996) Geometric constraints on potentially singular solutions for the 3D Euler equation Comm. *Partial Diff. Equns.* **21**, 559-571.

Constantin, P. (2008) Singular, weak and absent: Solutions of the Euler equations. *Proc. of the conference "Euler Equations 250 years on"* (Aussois June 2007), *Physica D* **237**, 1926–1931.

Constantin, P., Majda, A. J. & Tabak, E. (1994) Formation of strong fronts in the $2D$ thermal active scalar. *Nonlinearity* **7**, 1495-1533.

Constantin, P., Nie, Q., & Schorghofer, N. (1998), Nonsingular Surface Quasi-Geostrophic flows. *Phys. Lett. A* **24**, 168-172.

Córdoba, D. (1998) Nonexistence of simple hyperbolic blow-up for the quasi-geostrophic equation. *Ann,. Math* **148**, 1135-1152.

Córdoba, D. & Fefferman, Ch. (2001) Growth of solutions for QG and $2D$ Euler equations. *J. Amer. Math. Soc.* **15**, 665-670.

Córdoba, D., Fefferman, C. & Rodrigo, J., *Almost sharp fronts for the surface quasi-geostrophic equation*, *Proc. Natl. Acad. Sci.* **101(9)**, 2004.

Deng, J., Hou, T. Y. & Yu, X. (2005) Geometric Properties and Non-blowup of 3D Incompressible Euler Flow. *Commun. Partial Diff. Equns.* **30**, 225-243.

Deng, J., Hou, T. Y. & Yu, X. (2006) Improved geometric condition for non-blowup of the $3D$ incompressible Euler equation, *Commun. Partial Diff. Equns.* **31**, 293-306.

De Lellis, C. & Székelyhidi, L. (2007) The Euler equations as a differential inclusion. arXiv:math/0702079v3 [math.AP]

De Lellis, C. & Székelyhidi, L. (2008) On admissibility criteria for weak solutions of the Euler equations. arXiv:0712.3288v2 [math.AP]

ECMWF 2009 Large-scale Analyses : `http://www.met.rdg.ac.uk/Data/CurrentWeather`

Ertel, H. (1942) Ein Neuer Hydrodynamischer Wirbelsatz. *Met. Z.* **59**, 271–281.

Eyink, G. (2008) Dissipative Anomalies in Singular Euler Flows. Proc. of *Euler Equations 250 years on* held at Aussois June 2007, *Physica D*, **237**, 1956-1968.

Ferrari, A. (1993) On the blow-up of solutions of the 3D Euler equations in a bounded domain. *Comm. Math. Phys.* **155**, 277-294.

Foias, C., Manley, O., Rosa, R, & Temam R. (2001) *Navier-Stokes equations & Turbulence*, (Cambridge: Cambridge University Press).

Gibbon, J. D. (2008) *The three dimensional Euler equations: how much do we know?* Proc. of "Euler Equations 250 years on" Aussois June 2007, *Physica D*, **237**, 1894-1904.

Gibbon, J. D. and Holm, D. D. (2010) The dynamics of the gradient of potential vorticity, *J. Phys. A: Math. Theor.* **43**, 172001–8.

Grafke, T., Homann, H., Dreher, J. & Grauer, R. (2008) *Numerical simulations of possible finite time singularities in the incompressible Euler equations : comparison of numerical methods*, Proc. of "Euler Equations 250 years on" Aussois June 2007, **237**, 1932–1936.

Grauer, R., Marliani, C. & Germaschewski, K. (1998) Adaptive mesh refinement for singular solutions of the incompressible Euler equations. *Phys. Rev. Lett.* **80**, 4177-4180.

Grauer, R. & Sideris, T. (1991) Numerical computation of 3D incompressible ideal fluids with swirl. *Phys. Rev. Lett.* **67**, 3511–3514.

Gulak, Y. & Pelz, R. B. (2005) High-symmetry Kida flow: Time series analysis and resummation. *Fluid Dyn. Res.* **36**, 211–220.

Hamman, C. W., Klewick, J. C. & Kirby, R. M. (2008) On the Lamb vector divergence in Navier-Stokes flows. *J. Fluid Mech.* **610** 261-284.

Haynes, P. & McIntyre, M. E. (1987) On the evolution of vorticity and potential vorticity in the presence of diabatic heating and frictional or other forces. *J. Atmos. Sci.* **44**, 828–841.

Haynes, P. & McIntyre, M. E. (1990) On the conservation and impermeability theorems for potential vorticity. *J. Atmos. Sci.* **47**, 2021–2031.

Herring, J. K., Kerr, R. M. & Rotunno, R. (1994) Ertel's PV in stratified turbulence. *J. Atmos. Sci.* **51**, 35–47.

Holm, D. D. & Kupershmidt, B. (1983) Poisson brackets and Clebsch representations for magnetohydrodynamics, multi-fluid plasmas, and elasticity. *Physica D* **6**, 347–363.

Hoskins, B. J., McIntyre, M. E. & Robertson, A. W. (1985) On the use & significance of isentropic potential vorticity maps *Quart. J. Roy. Met. Soc.* **111**, 877–946.

Hou, T. Y. & Li, R, (2006) Dynamic Depletion of Vortex Stretching and Non-Blowup of the 3-D Incompressible Euler Equations. *J. Nonlinear Sci.* **16**, 639-664.

Hou, T. Y, & Li, R. (2008) *Blowup or No Blowup? The Interplay between*

Theory and Numerics Proc. of "Euler Equations 250 years on" Aussois June 2007, *Physica D* **237**, 1937-1944.

Kerr, R. M. (1993) Evidence for a singularity of the three-dimensional incompressible Euler equations. *Phys. Fluids A* **5**, 1725-1746.

Kerr, R. M. (2005a) Vorticity and scaling of collapsing Euler vortices. *Phys. Fluids A* **17**, 075103–114.

Kerr, R. M. (2005b) Vortex collapse. *Fluid Dyn. Res.* **36**, 249-260.

Kida, S. (1985) Three-Dimensional periodic flows with high-symmetry. *J. Phys. Soc. Jpn.* **54**, 2132-2136.

Kozono, H. & Taniuchi, Y. (2000) Limiting case of the Sobolev inequality in BMO, with applications to the Euler equations. *Comm. Math. Phys.* **214**, 191-200.

Kurgansky, M. V. & Pisnichenko, I. A. (2000) Modified Ertel's Potential Vorticity as a Climate Variable. *J Atmos Sci.* **57**, 822.

Kurgansky, M. V. & Tatarskaya, M. S. (1987) The potential vorticity concept in meteorology : A review. *Izvestiya - Atmospheric and Oceanic Physics* **23**, 587-606.

Kurgansky, M. V. (2002) *Adiabatic Invariants in large-scale atmospheric dynamics*, Taylor & Francis, London.

Lipnikov, K., Shashkov, M. & Yotov, I. (2009) Local flux mimetic finite difference methods, *Numer. Math.* **112**, 115-152.

Majda, A. J. & Bertozzi, A. L. (2001) *Vorticity and Incompressible Flow.* Cambridge University Press, Cambridge.

Marmanis, H. (1998) Analogy between the Navier-Stokes equations and Maxwell's equations : Application to turbulence. *Phys. Fluids* **10**, 1428-1437.

Moffatt, H. K. (1978) *Magnetic field generation in electrically conducting fluids* Cambridge University Press, Cambridge.

Morf, R. H., Orszag, S. A. & Frisch, U. (1980) Spontaneous singularity in three-dimensional, inviscid incompressible flow. *Phys. Rev. Lett.* **44**, 572–575.

Ohkitani, K. & M. Yamada, M. (1997) Inviscid and inviscid-limit behavior of a surface quasi-geostrophic flow. *Phys. Fluids* **9**, 876-882.

Ohkitani, K. (2008) A geometrical study of 3D incompressible Euler flows with Clebsch potentials – a long-lived Euler flow and its power-law energy spectrum. *Physica D* **237**, 2020-2027.

Orlandi, P. & Carnevale, G. (2007) Nonlinear amplification of vorticity in inviscid interaction of orthogonal Lamb dipoles. *Phys. Fluids* **19**, 057106.

Palmer, T. (1988) Analogues of potential vorticity in electrically conducting fluids *Geo. Astro. Fluid Dyn.*. **40** 133–145.

Pauls, W., Matsumoto, T., Frisch, U. & Bec, J. (2006) Nature of complex singularities for the two-dimensional Euler equation. *Physica D* **219**, 40-59.

Pelz, R. B. (1997) Locally self-similar, finite-time collapse in a high-symmetry vortex filament model. *Phys. Rev. E* **55**, 1617–1626.

Pelz, R. B. (2001) Symmetry and the hydrodynamic blow-up problem. *J. Fluid Mech.* **444**, 299-320.

Pelz, R. B. & Gulak Y. (1997) Evidence for a real-time singularity in hydrodynamics from time series analysis. *Phys. Rev. Lett.* **79**, 4998–5001.

Pelz, R. B. & Ohkitani, K. (2005) Linearly strained flows with and without boundaries – the regularizing effect of the pressure term Fluid. *Fluid Dyn.*

Res. **36**, 193-210.

Pumir, A. & Kerr, R. M. (1987) Numerical simulation of interacting vortex tubes. *Phys. Rev. Lett.* **58**, 1636-1639.

Pumir, A. & Siggia, E. (1990) Collapsing solutions to the 3D Euler equations. *Phys. Fluids A* **2**, 220–241.

Rodrigo, J. L. (2005) On the evolution of sharp fronts for the quasi-geostrophic equation. *Comm. Pure Appl. Math.* **58**, no. 6, 821–866.

Rousseaux, G., Seifer, S., Steinberg, V. & Wiebel A. (2007) On the Lamb vector and the hydrodynamic charge. *Exps. Fluids* **42**, 291-299.

Shnirelman, A. (1997) On the non-uniqueness of weak solution of the Euler equation. *Comm. Pure Appl. Math.* **50** 1260–1286.

Siggia, E. D. (1984) Collapse and amplification of a vortex filament. *Phys. Fluids* **28**, 794-805.

Sposito, G. (1997) On steady flows with Lamb surfaces *Int. J. Eng. Sci.*, **35**, 197-209.

Truesdell, C., & Toupin, R. A. (1960) *Classical Field Theories*, S. Flugge (ed.), Encyclopaedia of Physics III/1, Springer.